

Saddle-node ghost-induced low-frequency fluctuations in an external-cavity laser diode

F. Rogister,* P. Mégret, and M. Blondel

Service d'Electromagnétisme et de Télécommunications, Faculté Polytechnique de Mons, Boulevard Dolez 31, 7000 Mons, Belgium

(Received 16 August 2002; published 18 February 2003)

We investigate numerically the low-frequency fluctuation regime in a laser diode subject to optical feedback. We demonstrate that a saddle-node ghost can induce this regime.

DOI: 10.1103/PhysRevE.67.027202

PACS number(s): 42.65.Sf, 42.60.Mi, 42.55.Px

I. INTRODUCTION

A semiconductor laser subject to optical feedback exhibits a large variety of dynamical instabilities including chaos. These can lead to severe degradation of the laser characteristics, e.g., the increase of its typical optical linewidth from 100 MHz to several tens of gigahertz (see Ref. [1] and references therein). When the laser diode is pumped close to its solitary threshold, its optical power can exhibit sudden dropouts that occur aperiodically. The typical duration between two consecutive dropouts is much larger than the period of the relaxation oscillations or the external-cavity round-trip time. For this reason, this regime is usually referred to as the low-frequency fluctuation (LFF) regime. Already reported in 1977 by Risch and Vourmard [2], the LFF regime has attracted much theoretical and experimental interest. Multiple explanations of its origin have been proposed. A widely accepted interpretation of this phenomenon was presented by Sano [3] in 1994; it relies on the Lang-Kobayashi equations [4] that assume single-mode operation of the laser and weak to moderate amount of external optical feedback. Sano showed that the intensity dropouts are caused by crises between local chaotic attractors and saddle-type antimodes [3]. In his analysis, the process of intensity recoveries is associated to a chaotic itinerancy of the system trajectory in phase space among attractor ruins of external-cavity modes (ECMs), with a drift towards the maximum gain mode close to which collisions of the attractor ruins of ECMs and antimodes occur.

Contrary to the single-feedback case, the dynamics of a laser diode subject to two optical feedbacks has been poorly investigated although its study reveals a great wealth of dynamical behaviors. Fischer *et al.* have reported experimental realization of high-dimensional chaos in such a system [5]. Rogister *et al.* [6,7] have numerically and experimentally demonstrated that a laser diode subject to a single optical feedback and operating in the low-frequency fluctuation regime can be stabilized by means of a second optical feedback. This method relies on the destruction of saddle-type antimodes responsible for the LFF crises and the creation of new, stable, maximum gain modes onto which the laser locks. The idea of using a second optical feedback to stabilize an external-cavity laser diode was proposed for the first time by Liu and Ohtsubo in Ref. [8] but in the case of a laser pumped far above threshold. In this case, however, the physi-

cal mechanisms underlying the laser stabilization are still unknown [8]. Furthermore, the experimental study on the double-feedback configuration has revealed time-periodic oscillations with frequencies much larger than those that might *a priori* be expected when the laser is biased close to threshold. Periodic oscillations with similar frequencies have been found by investigating numerically the Lang-Kobayashi equations extended to the double-feedback configuration. They have been interpreted as resulting from a beating between ECMs and antimodes [9,10].

In this paper, we investigate the dynamics of a semiconductor laser pumped close to its solitary threshold and subject to two optical feedbacks. The increase of one of the feedback rates leads to the destruction of pairs of steady-state solutions. However, even when they have disappeared, the fixed points continue to influence the dynamics of the system. We demonstrate that these saddle-node ghosts can initiate the intensity dropouts that characterize the low-frequency fluctuation regime.

II. MODEL AND STEADY-STATE SOLUTIONS

The Lang-Kobayashi equations [4] can be extended to the problem of a laser diode subject to optical feedback from a double cavity (see Fig. 1) by including a second delay term in the rate equation for the electric field. Using the same normalization as in Ref. [11], the modified Lang-Kobayashi equations are

$$\frac{dE}{ds} = (1 + i\alpha)NE + \kappa_1 E(s - \tau_1) \exp(-i\Omega\tau_1) + \kappa_2 E(s - \tau_2) \exp(-i\Omega\tau_2), \quad (1)$$

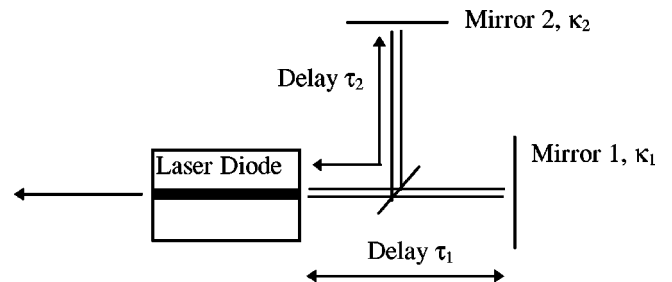


FIG. 1. Schematic configuration of a laser diode subject to optical feedback from a double cavity.

*Corresponding author. Email address: rogister@telecom.fpms.ac.be

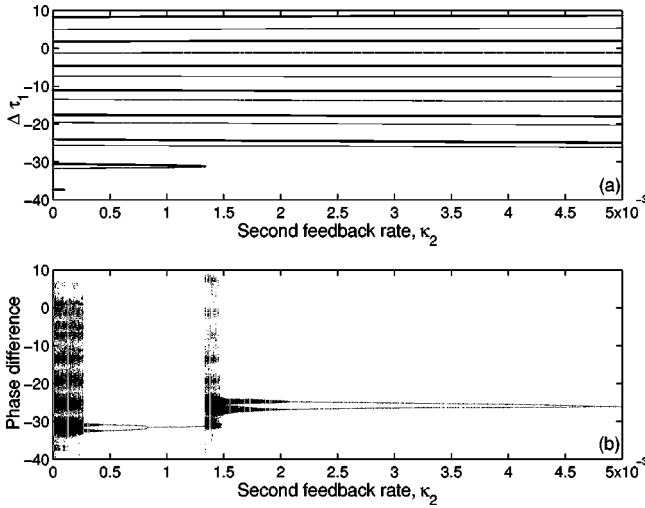


FIG. 2. (a) Stationary angular frequencies Δ as function of κ_2 . Thin curves correspond to ECMs, thick curves to antimodes. (b) Bifurcation diagram of the phase difference function. The first feedback rate is $\kappa_1 = 7.2 \times 10^{-3}$.

$$T \frac{dN}{ds} = P - N - (1 + 2N)|E|^2. \quad (2)$$

The dimensionless time s is measured in units of the photon lifetime τ_p ; $E(s) = A(s) \exp[i\phi(s)]$ and $N(s)$ are the normalized slowly varying complex electric field and the normalized excess carrier number. κ_1 and κ_2 are the normalized feedback rates of the first and second external cavities and τ_1 and τ_2 the ratios of the round-trip time to the photon lifetime for those cavities. α is the linewidth enhancement factor and Ω is the product of the angular frequency of the solitary laser and the photon lifetime. P is the dimensionless pumping current above solitary laser threshold and T the ratio of the carrier lifetime to the photon lifetime.

The steady-state solutions of Eqs. (1) and (2) can be written in the form

$$E = A_s \exp[i(\Delta - \Omega)s], \quad (3)$$

where the stationary angular frequency Δ , the amplitude A_s and the normalized carrier number N_s satisfy the equations

$$\begin{aligned} \Delta &= \Omega - \kappa_1 [\alpha \cos(\Delta \tau_1) + \sin(\Delta \tau_1)] \\ &\quad - \kappa_2 [\alpha \cos(\Delta \tau_2) + \sin(\Delta \tau_2)], \end{aligned} \quad (4)$$

$$A_s^2 = \frac{P - N_s}{1 + 2N_s} \geq 0, \quad (5)$$

and

$$N_s = -\kappa_1 \cos(\Delta \tau_1) - \kappa_2 \cos(\Delta \tau_2). \quad (6)$$

In the following, we use typical values for the linewidth enhancement factor and the ratio of the carrier lifetime to the photon lifetime, namely, $\alpha = 4$ and $T = 1000$, and we assume that the laser works at the wavelength $\lambda = 780$ nm and is pumped at threshold (i.e., $P = 0$). Figure 2(a), which is ob-

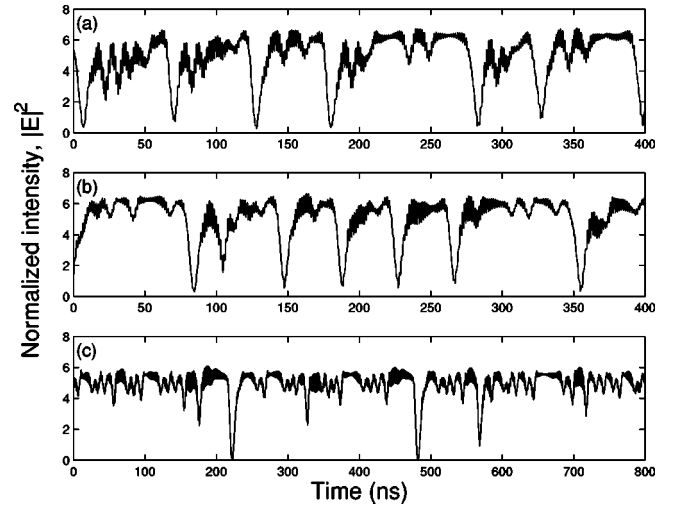


FIG. 3. Time traces of the normalized laser intensity for $\kappa_2 = 0$ (a), 1.6×10^{-4} (b), and 1.4×10^{-3} (c). $\kappa_1 = 7.2 \times 10^{-3}$. The time traces have been averaged over 4 ns to model the limited bandwidth of detectors that are usually employed in experiments.

tained from Eq. (4), shows typical evolutions of the product $\Delta \tau_1$ of the stationary angular frequencies (Δ) and the first feedback delay (τ_1) when κ_2 is varied. The figure is calculated for $\kappa_1 = 7.2 \times 10^{-3}$, $\tau_1 = 1400$, $\tau_2 = 1267 + 1.5 \times \lambda / (2c\tau_p)$, where $\tau_p = 1$ ps is the photon lifetime and c the velocity of light in vacuum, with κ_2 as the bifurcation parameter.

For these numerical values, the phase differences over one round trip in the first and the second cavities are approximately $\Omega \tau_1 \cong -2.90 \text{ mod } 2\pi$ and $\Omega \tau_2 \cong 2.78 \text{ mod } 2\pi$, respectively. Similarly to the single-feedback case (see Ref. [1]), the steady-state solutions are of two kinds: saddle points that are referred to as antimodes and other solutions that can be stable and are called external cavity modes. Figure 2(a) shows that several pairs of external-cavity modes and antimodes collide and disappear through saddle-node bifurcations as the rate of the second feedback increases. Further, increases of κ_2 lead to the creation of new pairs of steady-state solutions but those are not shown in the figure.

III. NUMERICAL RESULTS

In this section, the bifurcation diagram of the phase difference function $\phi(t) - \phi(t - \tau_1) + \Omega \tau_1$ [Fig. 2(b)], the temporal evolution of the intensity $|E|^2$ (Fig. 3) and the system trajectories in the plane $[\phi(t) - \phi(t - \tau_1) + \Omega \tau_1, N(t)]$ (Figs. 4 and 5) are calculated by solving numerically Eqs. (1) and (2). The choice of the phase difference function is convenient because it reduces to $\Delta \tau_1$ for stationary behaviors. We can, therefore, compare Fig. 2(a) and Fig. 2(b). When the first cavity is acting alone, i.e., $\kappa_2 = 0$, the trajectory displays chaotic itinerancy among seven attractor ruins of external cavity modes and collisions with three different antimodes [Fig. 4(a)]. Sharp intensity dropouts are clearly visible in Fig. 3(a). For $\kappa_2 = 1.2 \times 10^{-4}$, the ECM with the lowest

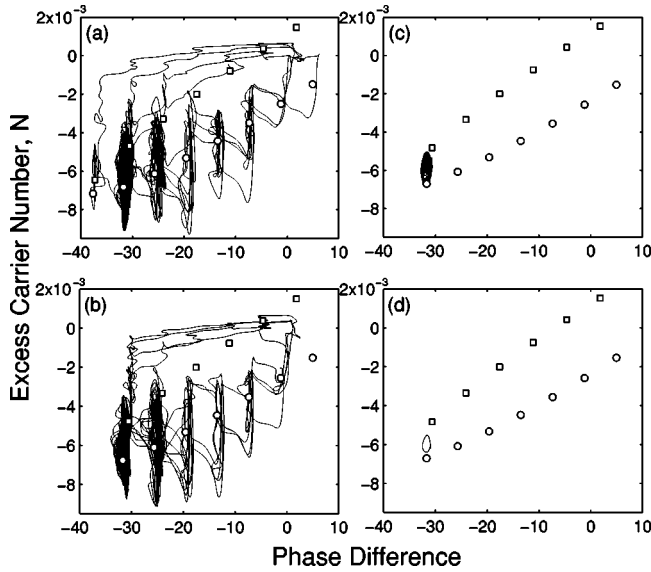


FIG. 4. Phase trajectories observed in the plane $[\phi(t) - \phi(t - \tau_1) + \Omega \tau_1, N(t)]$. Squares show the antimodes; circles the external-cavity modes. (a) and (b): LFF for $\kappa_2 = 0$ and $\kappa_2 = 1.6 \times 10^{-4}$, respectively. (c) Chaotic behavior for $\kappa_2 = 2.8 \times 10^{-4}$. (d) Limit cycle corresponding to a periodic behavior for $\kappa_2 = 4.5 \times 10^{-4}$. The first feedback rate is $\kappa_1 = 7.2 \times 10^{-3}$ in all cases.

frequency and the corresponding antinode collide and disappear through a saddle-node bifurcation (Fig. 2). The LFF continues however [Fig. 3(b)], because a crisis with remaining antimodes still occur [Fig. 4(b)]. As κ_2 increases further, the ruin of the chaotic attractor associated to the lowest-frequency external-cavity mode decreases progressively in

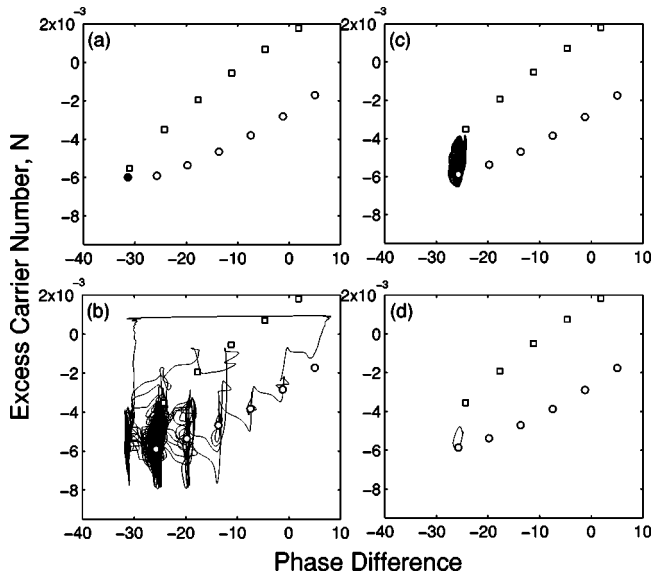


FIG. 5. Phase trajectories observed in the plane $[\phi(t) - \phi(t - \tau_1) + \Omega \tau_1, N(t)]$. Squares show the antimodes; circles the external-cavity modes. (a) Stationary behavior for $\kappa_2 = 1.3 \times 10^{-3}$, the laser locks onto the lowest-frequency ECM (filled circle). (b) Atypical LFF for $\kappa_2 = 1.4 \times 10^{-3}$. (c) Chaotic behavior for $\kappa_2 = 1.6 \times 10^{-3}$. (d) Limit cycle for $\kappa_2 = 2.2 \times 10^{-3}$. The first feedback rate is $\kappa_1 = 7.2 \times 10^{-3}$ in all cases.

size. For $\kappa_2 = 2.6 \times 10^{-4}$, the attractor does no longer collide with the saddle-point. Chaotic, quasiperiodic and periodic behaviors are successively observed from $\kappa_2 = 2.6 \times 10^{-4}$ to 8.4×10^{-4} . As an example, a stable chaotic attractor and a limit cycle are shown in Figs. 4(c), 4(d) for $\kappa_2 = 2.8 \times 10^{-4}$ and $\kappa_2 = 4.5 \times 10^{-4}$, respectively. At $\kappa_2 = 8.4 \times 10^{-4}$, the lowest-frequency ECM becomes stable through a Hopf bifurcation. From $\kappa_2 = 8.4 \times 10^{-4}$ to 1.34×10^{-3} , all trajectories are attracted by this stable point regardless of the initial conditions. As κ_2 increases, the ECM and the antinode come close to each other and finally collide at $\kappa_2 = 1.34 \times 10^{-3}$ (Fig. 2) and disappear. Figure 5(a) shows the steady-state solutions just before the saddle-node bifurcation. As this pair of steady-state solutions disappears, an atypical LFF is observed; the trajectory in phase space exhibits a chaotic itinerancy among the external-cavity modes with a drift toward the lowest frequencies. The fixed points that have disappeared at $\kappa_2 = 1.34 \times 10^{-3}$ continue to influence the dynamics: they leave a ghost that attracts the trajectory (features of saddle-node ghost are described in Refs. [12,13]). The trajectory is then repelled toward higher values of the excess carrier number along the direction of the unstable manifold of the antinode that has disappeared [Fig. 5(b)]. As a result, the laser exhibits strong intensity dropouts [Fig. 3(c)] that are not associated to attractor crises. Additional increase of κ_2 leads to a progressive attenuation of the influence of the annihilated fixed points on the dynamics as well as to a decrease in size of the ruin of the nearest chaotic attractor. Chaotic [Fig. 5(c)], quasiperiodic and periodic [Fig. 5(d)] behaviors are successively observed. Finally, at $\kappa_2 = 4.8 \times 10^{-3}$ the laser output becomes stationary. For $\kappa_2 \geq 4.8 \times 10^{-3}$, the rest of the bifurcation diagram reveals a scenario similar to that described in Refs. [6,7], i.e., a succession of regions within which the laser is locked onto a stable maximum gain mode and regions where the laser exhibits complex behaviors such as chaos and low-frequency fluctuations.

IV. CONCLUSION

By using an extension of the Lang-Kobayashi equations, we have investigated the dynamics of a laser diode subject to optical feedback from a double cavity and pumped at threshold. When both cavities are acting in concert, an increase of one of the feedback rate can lead to the annihilations of fixed points through saddle-node bifurcations. We have shown that the saddle-node remnants continue to influence the dynamics and can induce intensity dropouts. This kind of solution have not been reported so far in the extensively studied single-feedback case. We attribute the difficulty to observe such dynamics in a single-feedback system to the fact that, in this system, an increase of the feedback rate does never lead to the annihilation of fixed points even when multiple round trips in the single external cavity are taken into account in the Lang-Kobayashi equations. In the double-feedback configuration, annihilation of pairs of external-cavity modes and antimodes can be achieved regardless of the lengths of the external cavities and in large ranges of feedback phases. In each case, a second optical feedback strongly modifies the

pattern of the steady-state solutions and leads to the destruction of some of them. However, the second feedback phase has to be adequately tuned in order to lead to annihilation of the steady-state solutions with the lowest frequencies, of which the remnants can induce atypical LFF.

ACKNOWLEDGMENTS

This research was supported by the InterUniversity Attraction Pole (IAP V/18) program of the Belgian government and the Fonds National de la Recherche Scientifique.

-
- [1] J. Mork, B. Tromborg, and J. Mark, *IEEE J. Quantum Electron.* **28**, 93 (1992).
 - [2] C. Risch and C. Vourmard, *J. Appl. Phys.* **48**, 2083 (1977).
 - [3] T. Sano, *Phys. Rev. A* **50**, 2719 (1994).
 - [4] R. Lang and K. Kobayashi, *IEEE J. Quantum Electron.* **16**, 347 (1980).
 - [5] I. Fischer, O. Hess, W. Elsässer, and E. Göbel, *Phys. Rev. Lett.* **73**, 2188 (1994).
 - [6] F. Rogister, P. Mégret, O. Deparis, M. Blondel, and T. Erneux, *Opt. Lett.* **24**, 1218 (1999).
 - [7] F. Rogister, D.W. Sukow, A. Gavrielides, P. Mégret, O. Deparis, and M. Blondel, *Opt. Lett.* **25**, 808 (2000).
 - [8] Y. Liu and J. Ohtsubo, *IEEE J. Quantum Electron.* **33**, 1163 (1997).
 - [9] F. Rogister, Ph.D. thesis, Faculté Polytechnique de Mons, 2001 (unpublished).
 - [10] D.W. Sukow, M.C. Hegg, J.L. Wright, and A. Gavrielides, *Opt. Lett.* **27**, 827 (2002).
 - [11] G. Lythe, T. Erneux, A. Gavrielides, and V. Kovanis, *Phys. Rev. A* **55**, 4443 (1999).
 - [12] J.M.T. Thomson and H.B. Stewart, *Nonlinear Dynamics and Chaos* (Wiley, Chichester, 1986).
 - [13] S.H. Strogatz, *Nonlinear Dynamics and Chaos: With Applications to Physics, Biology, Chemistry and Engineering* (Addison-Wesley, Reading, Massachusetts, 1994).